

the Fourier transform of a cosine function) with a Lorentzian function (the Fourier transform of an exponential function).

3. Parseval's theorem: The total energy of a function in the time domain/spatial domain is the same as the total energy of the Fourier transform of that function in the frequency domain/spatial frequency domain:

$$\begin{aligned}\int_{-\infty}^{\infty} |s(t)|^2 dt &= \int_{-\infty}^{\infty} |S(f)|^2 df \\ \int_{-\infty}^{\infty} |\rho(x)|^2 dx &= \int_{-\infty}^{\infty} |S(k)|^2 dk\end{aligned}\quad (\text{A.12})$$

example of Parseval's theorem can also be found in NMR, in which the amplitude of the signal directly after an RF pulse is proportional to the integrated area of the IR spectrum after Fourier transformation.

4. Scaling law: If a time-domain signal is expanded by some factor, then its Fourier transform is compressed by the same factor:

$$s(at) \Leftrightarrow \frac{1}{|a|} S\left(\frac{f}{a}\right) \quad (\text{A.13})$$

example, in MRI, if the  $T_2^*$  value of tissue is increased through better shimming, time-domain signal decays to zero more slowly, and the corresponding frequency-domain spectrum is narrower.

## Appendix B

# Backprojection and Filtered Backprojection

### B.1. INTRODUCTION

The problem of reconstructing a two-dimensional image from a series of one-dimensional projections is common to a number of imaging modalities. Of those covered in this book, CT, SPECT, and PET produce data exclusively as a series of projections, and, less commonly, MRI projection reconstruction sequences are used, typically for imaging samples with very short  $T_2$  values. In each of these methods a number of one-dimensional projections,  $p_1, p_2, \dots, p_n$ , are acquired with the detector oriented at different angles with respect to the object, as shown in Figure B.1. In the following analyses, the object is represented as a function  $f(x, y)$ , in which the spatially dependent values of  $f$  correspond to the distribution of radiopharmaceutical in SPECT or PET or attenuation coefficients in X-ray CT.

The coordinate system in the measurement frame is represented by  $(r, s)$ , where  $r$  is the direction parallel to the detector and  $s$  is the direction along the ray sum at  $90^\circ$  to the  $r$  dimension. The angle between the  $x$  and  $r$  axes is denoted as  $\phi$ , and so by simple trigonometry

$$\begin{aligned}r &= x \cos \phi + y \sin \phi \\ s &= -x \sin \phi + y \cos \phi\end{aligned}\quad (\text{B.1})$$

The measured projection is denoted by  $p(r, \phi)$ . Projections are acquired at different values of  $\phi$  until coverage over a range of  $180^\circ$  or  $360^\circ$ , depending upon the particular application, has been reached. A number of schemes exist for the reconstruction of the image, covered in the following sections.

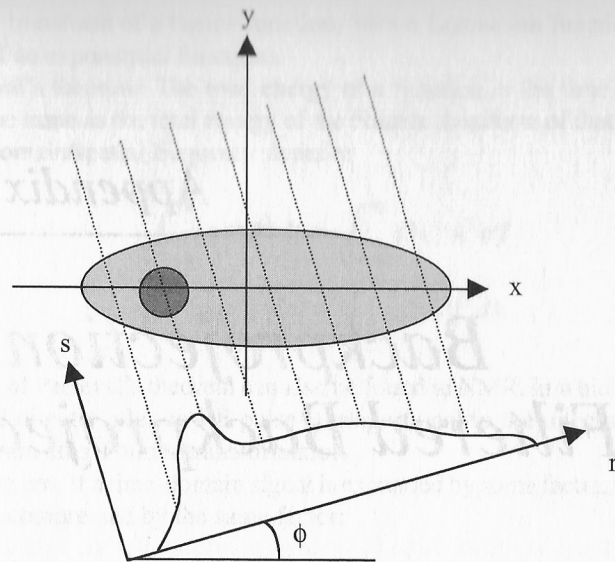


**FIGURE B.1.** The coordinate system used for analyzing backprojection algorithms. The object can be represented as  $f(x, y)$ , where  $x$  and  $y$  represent the image coordinates. Successive projections of the object are obtained with the detector aligned at different values of the angle  $\phi$ .

## B.2. BACKPROJECTION

Simple backprojection of the acquired projections corresponds to direct implementation of the inverse Radon transform. Backprojection assigns an equal weighting to the pixels contributing to each point in a particular projection. This process is repeated for all of the projections, and the pixel intensities are summed to give the reconstructed image  $\hat{f}(x, y)$ . Mathematically,  $\hat{f}(x, y)$  can be represented as

$$\hat{f}(x, y) = \sum_{j=1}^n p(r_j, \phi_j) d\phi_j \quad (\text{B.2})$$

where  $n$  is the number of projections. Figure B.2 shows the typical artifacts associated with simple backprojection.

The backprojected image of a well-known model of the head, the Shepp–Logan phantom, is shown in Figure B.3. This phantom is often used to assess the effect of newly developed reconstruction algorithms and consists of a set of ellipses: the largest outer ellipse represents the head, with smaller ellipses representing features within the head. Notice that, in addition to blurring the edges of the image, the contrast within the phantom is also greatly reduced by simple backprojection.

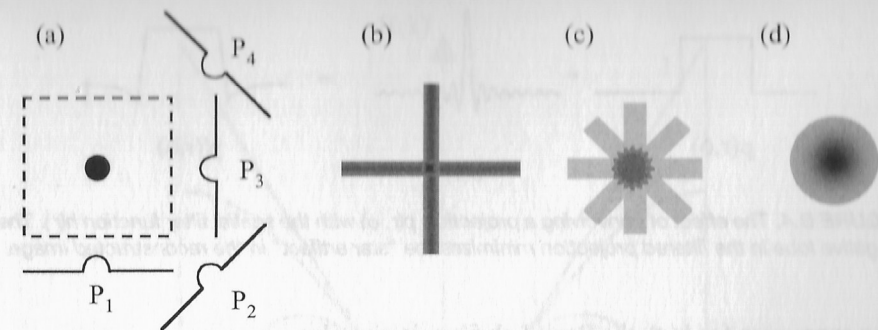


**FIGURE B.2.** (a) A series of projections  $P_1$ – $P_4$  acquired for a simple circular object. The dashed lines represent the FOV of the image. (b) A simple backprojection reconstruction using only projections  $P_1$  and  $P_3$ . (c) The “star artifact” produced by the reconstruction of a moderate number of projections. (d) The radial blurring produced using simple backprojection of an infinite number of projections.

## B.3. FILTERED BACKPROJECTION

The widely implemented method of filtered backprojection consists in applying a filter to each projection before backprojection in order to reduce the artifacts associated with simple backprojection. One of the most common implementations uses the Ramachandran–Lakshminarayanan (Ram–Lak) filter. If the filter is applied in the spatial domain, then the filtered projection  $p'(r, \phi)$  can be represented as

$$p'(r, \phi) = p(r, \phi) * h(r) \quad (\text{B.3})$$

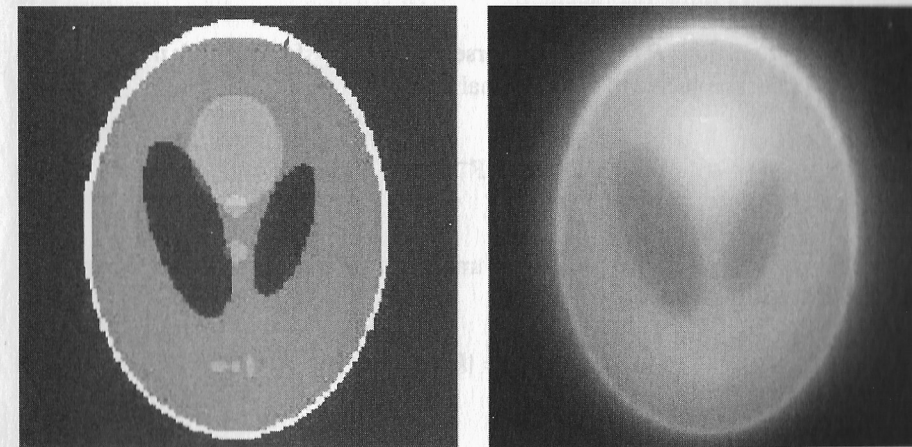


**FIGURE B.3.** An image (right), obtained using backprojection, of the Shepp–Logan phantom (left) shows considerable blurring and contrast loss.

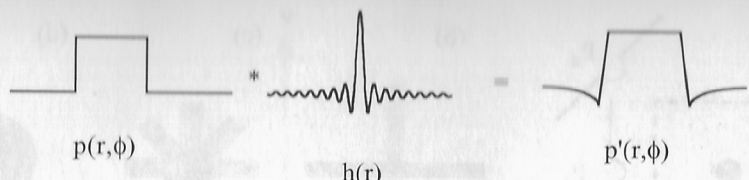


**FIGURE B.4.** The effect of convolving a projection  $p(r, \phi)$  with the spatial filter function  $h(r)$ . The negative lobe in the filtered projection minimizes the “star artifact” in the reconstructed image.

The expression for  $h(r)$ , the Ram–Lak filter, is given by

$$h(r) = \frac{1}{2(dr)^2} \left[ \text{sinc}\left(\frac{r}{dr}\right) \right] - \frac{1}{4(dr)^2} \left[ \text{sinc}^2\left(\frac{r}{2dr}\right) \right] \quad (\text{B.4})$$

where  $dr$  is the sampling interval along the  $r$  axis. The form of  $h(r)$  is shown in Figure B.4. After filtering, the projections are then backprojected as described previously. The major effect of the convolution of  $p(r, \phi)$  with  $h(r)$  is to decrease the intensity of the “star artifact” produced by simple backprojection.

Because the mathematical process of convolution is computationally intensive, in practice filtered backprojection is carried out in the spatial frequency domain using fast Fourier transform methods. Convolution in the spatial domain is equivalent to multiplication in the spatial frequency domain, and multiplication can be performed much faster computationally than convolution. Each projection  $p(r, \phi)$  is Fourier-transformed along the  $r$  dimension to give  $P(k, \phi)$ , and then  $P(k, \phi)$  is multiplied by  $H(k)$ , the Fourier transform of  $h(r)$ , to give  $P'(k, \phi)$ :

$$P'(k, \phi) = P(k, \phi)H(k) \quad (\text{B.5})$$

The filtered projections  $P'(k, \phi)$ , are inverse-Fourier-transformed back into the spatial domain and backprojected to give the final image  $\hat{f}(x, y)$ :

$$\hat{f}(x, y) = \sum_{j=1}^n \mathbb{F}^{-1}\{P'(k, \phi_j)\} d\phi \quad (\text{B.6})$$

where  $\mathbb{F}^{-1}$  represents an inverse Fourier transform. The expression for  $H(k)$  in equation (B.5) is given by

$$H(k) = |k| \text{ rect}(k) \quad (\text{B.7})$$

where:

$$\begin{aligned} \text{rect}(k) &= 1 && \text{if } |k| \leq 0.5 \\ &= -1 && \text{if } |k| \geq 0.5 \end{aligned} \quad (\text{B.8})$$

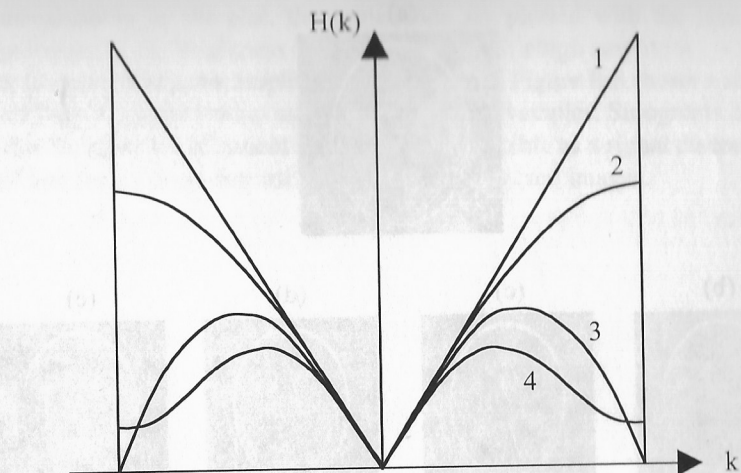


**FIGURE B.5.** Some common filter functions used for backprojection. 1, Ram–Lak; 2, Shepp–Logan; 3, low-pass cosine; and 4, generalized Hamming.

The form of  $H(k)$  in the spatial frequency domain is shown in Figure B.5. As can be appreciated, this filter does not have very desirable noise characteristics because it amplifies high spatial frequencies. In order to improve the noise performance of the filter, the amplification of high spatial frequencies can be reduced, resulting in commonly used functions such as Shepp–Logan, low-pass cosine, or generalized Hamming filters, which are also shown in Figure B.5.

Figure B.6 compares the results of filtered backprojection of the Shepp–Logan phantom with a Ram–Lak and a Hamming filter.

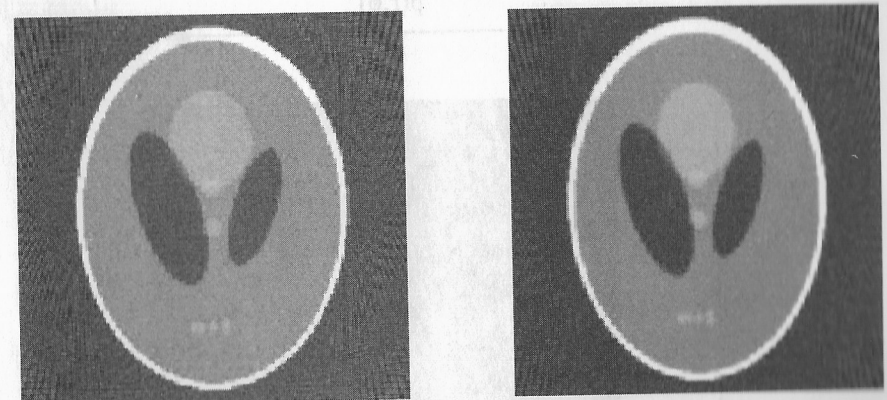


**FIGURE B.6.** Filtered backprojections of the Shepp–Logan phantom using (left) the Ram–Lak filter and (right) a generalized Hamming filter. Results using the Hamming filter give a higher SNR image, but one which is also more blurred.

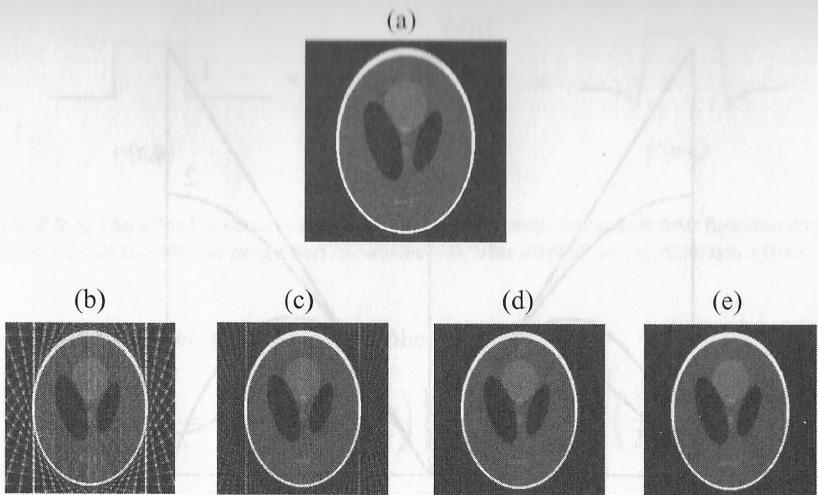


**FIGURE B.7.** The effect of the number of projections on the final image using filtered backprojection with a Shepp–Logan filter. (a) The original Shepp–Logan phantom. (b–e) The effect of increasing the number of projections for reconstruction: (b) 20 projections, (c) 45 projections, (d) 90 projections, and (e) 180 projections.

An important data acquisition parameter is the number of projections required to produce a high-quality image. If too few projections are acquired, then significant image artifacts occur in data reconstruction. Figure B.7 shows examples of these so-called “streak” artifacts.

A common method of displaying projection data is called a sinogram, in which the projections are plotted as a function of the angle  $\phi$ . In order to reduce the

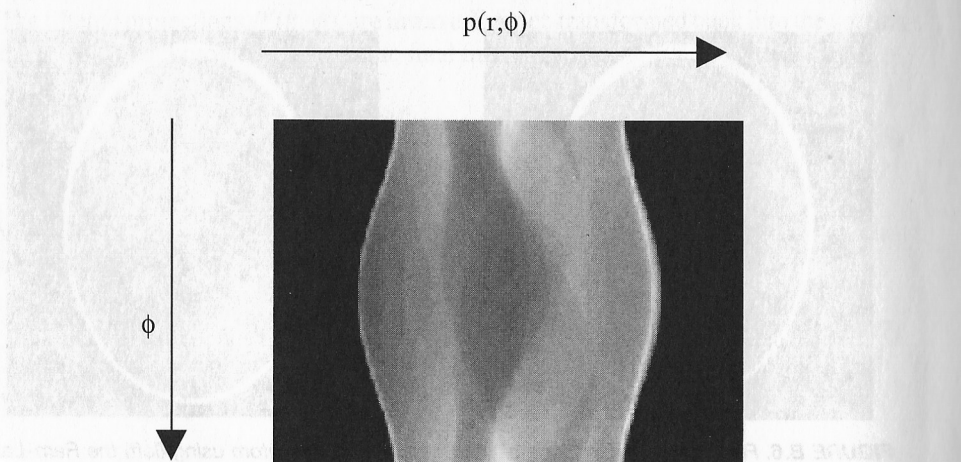


**FIGURE B.8.** Sinogram from a Shepp–Logan phantom.

dimensionality of the plot, the projections are plotted with the signal amplitude represented by the brightness of the sinogram, with a high amplitude corresponding to a bright pixel and a low amplitude to a dark pixel. Figure B.8 shows a sinogram from the Shepp–Logan phantom used in the previous examples. Sinograms can be used to detect the presence of patient motion, which is visible as a signal discontinuity. Such motions can cause severe artifacts in the reconstructed images.